Inorganica Chimica Acta, 35 (1979) 165–175

Metalloprotein Models, Location of the Magnetic Axes in Low-Symmetry Complexes. Single Crystal Electron Paramagnetic Resonance, Magnetic Susceptibility Anisotropy, and Angular Overlap Ligand Field Calculations on a Complex containing the Distorted Tetrahedral $Co^{II}N_2O_2$ Coordination Unit, Bis(N-isopropylsalicyclaldiminato)cobalt(II)

WILLIAM DeW. HORROCKS, Jr.* and DOMINICK A. BURLONE

Grover Cleveland Chandlee Laboratory, Department of Chemistry, The Pennsylvania State University, University Park, Pa. 16802, U.S.A.

Received December 2, 1978

Single-crystal and powder electron paramagnetic resonance (epr) spectra of bis(N-isopropylsalicylaldiminato)cobalt(II), Co(iPr-sal)$_2$, doped into the isomorphous zinc complex were obtained at liquid helium temperatures. Principal molecular g-values of g_x, 7.09; g_y, 0.57; and g_z, <0.3, were obtained. The orientation of the principal magnetic axes with respect to the distorted tetrahedral $Co^{II}N_2O_2$ coordination unit of approximate C_2 symmetry was determined from the angular variation of the single-crystal epr signals using the method of Schonland. The x-axis approximately bisects the N–Co–O angles of the individual bidentate ligands, the y-axis is the approximate bisector of the N–Co–O angles formed between different ligands, while the z-axis is taken as the approximate molecular C_2 axis. Ligand field calculations employing the angular overlap model (AOM) predict principal molecular magnetic axis directions in excellent agreement with experiment. Principal crystal magnetic susceptibility anisotropies were measured by the critical torque method. The derived molecular susceptibilities were used to evaluate dipolar nuclear magnetic resonance shifts of ligand nuclei. When dipolar contributions to the observed shifts are accounted for, the unpaired electron spin delocalization patterns of the Co(iPr-sal)$_2$ and Ni(iPr-sal)$_2$ are quite similar. The relevance of these results to the problem of achieving a detailed understanding of the properties of cobalt(II)-substituted zinc metalloproteins is stressed.

Introduction

Zinc-containing enzymes are ubiquitous in nature [1, 2]. The metal-ion is required for activity in this class of enzyme and is generally thought to reside at the active site. Unfortunately zinc is a colorless, diamagnetic ion unsuitable for most spectroscopic investigations. It has been found, however, that many divalent ions with more favorable spectroscopic properties can replace zinc, often with retention of at least partial catalytic activity. Of the divalent metal ion replacements, manganese(II) [3] and cobalt(II) [4] have been the most useful as reporter ions in the study of zinc metalloproteins. For cases where it has been firmly established *via* X-ray crystallographic studies, the zinc ion has been found to be 4-coordinate with a distorted tetrahedral ZnN_2O_2 (carboxypeptidase [5], thermolysin [6]), ZnN_3O (carbonic anhydrase [7]), $ZnNS_3$, or ZnS_4 (alcohol dehydrogenase [8]) coordination polyhedron. For all of the above examples it has been found possible to substitute cobalt(II) for zinc with retention of partial (or enhancement of) activity. In order to extract maximum information from studies of metal-substituted enzymes it is necessary to have a detailed understanding of the spectral and magnetic properties of the coordination units in question. Such information can be obtained through the study of model complexes. For this reason we have undertaken a program of investigation of distorted tetrahedral cobalt(II) complexes involving various combinations of ligand atoms found in metalloproteins.

Our concern here is with a model for the distorted tetrahedral CoN_2O_2 coordination unit. The term model is used advisedly, for the substance we have studied, bis(N-isopropylsalicylaldiminato)cobalt(II), Co(iPr-sal)$_2$, **1** of course, exhibits no catalytic activity, nor does it represent an exact replica of the coordination site in a metalloenzyme. It does, however, have certain features in common with the

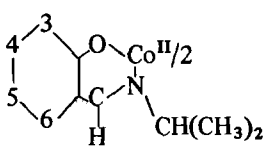

1

*Author to whom correspondence should be addressed.

CoN_2O_2 unit in metalloproteins, namely, a distorted tetrahedral coordination sphere and a like set of ligand atoms. For the present purposes $Co(iPr\text{-}sal)_2$ has the advantage that the crystal structure [9] of the isomorphous [10] nickel(II) complex is known and we were able to carry out the detailed physical studies described here.

Cobalt(II) has proved to be particularly useful as a reporter ion in that it can be studied by a variety of physical techniques. In a distorted tetrahedral environment it exhibits reasonably intense absorptions in the visible region allowing it to be studied by circular dichroism [11], CD, and magnetic CD [12] as well as by absorption spectroscopy [13]. These absorption characteristics have also been exploited in internal energy transfer distance measurements [14, 15]. The cobalt(II) ion is paramagnetic and therefore amenable to study by magnetic susceptibility methods and electron paramagnetic resonance, epr, spectroscopy. It is also potentially useful as a nuclear magnetic resonance, nmr, shift and relaxation probe. A detailed examination of the magnetic properties (g- and susceptibility-tensors) and their relationship to the structure of the coordination sphere is the topic of principal concern to us in this paper. Heretofore, analysis of the epr spectra of cobalt(II) substituted zinc metalloenzymes has depended upon semiquantitative comparisons with results obtained on model complexes of known structures [16]. The application [17] of phenomenological ligand field theory to such low-symmetry situations has not been particularly rewarding. The epr experiments have generally been carried out on powders or frozen solutions which yield no information regarding the orientation of the g-tensor with respect to the ligand field experienced by the metal ion.

In order to gain further insight into the factors which determine the details of the magnetic properties of low-symmetry cobalt(II) complexes, we have undertaken a program of single crystal epr and magnetic susceptibility anisotropy studies of complexes of this type. In addition we have been developing [18] a theoretical methodology, involving the application of the angular overlap model, AOM, to analyze in detail the experimental results. Our initial results, as well as recent work of others [19, 20], suggest that AOM calculations may be capable of predicting the directions of the principal magnetic axes in situations where these are not determined by symmetry. Our theoretical approach is capable of providing an invaluable link between the structure of the first coordination sphere and the ground state magnetic properties of highly distorted complexes.

Knowledge of the directions of the magnetic axes and the magnitudes of the principal magnetic susceptibilities, together with the structure of a complex, allows the evaluation of dipolar contributions to nmr shifts of ligand nuclei [21–25]. Structural information on small molecules contained in dipolar shifts has been exploited in the lanthanide shift reagent area [26]. Structural assessments on biological macromolecules have been attempted based on nmr dipolar shifts induced by protein-bound lanthanide ions [27] and in low-spin iron(III) heme proteins [28]. The present evaluation of dipolar shifts in a model complex has been made in order to gain insight into the possible use of cobalt(II) as an nmr shift probe in substituted zinc metalloproteins.

Experimental

The complexes $M(iPr\text{-}sal)_2$, M = Co, Zn were synthesized according to a literature method [29] from the pre-formed Schiff base and metal salt in the presence of acetate ion in ethanol solution. They were recrystallized from isopropanol–chloroform. Single crystals of the zinc complex containing 0.5–1.0 mol percent of the cobalt compound were grown by slow evaporation of chloroform solutions.

Single doped crystals were mounted (Elmer's glue) on cylindrical teflon plugs constructed so as to slip over the end of a quartz rod for the crystal rotation experiments. The crystal allignment on the teflon plug was checked by X-ray oscillation photography using a Weissenberg camera. Only mountings within 3° of one of the principal crystallographic axes of the orthohombic unit cell were used for the epr experiments. The epr experiments were carried out using a Varian E-line spectrometer equipped with a 12 in electromagnet operating at 9 GHz. Rotation of the single crystals was accomplished using a Varian attachment constructed for the purpose. The powder spectrum was obtained using a finely pulverized sample of the doped material contained in a quartz tube. All epr experiments were carried out at 4.2 K using a liquid helium dewar. The field sweep was calibrated using a proton resonance probe and was found to be accurate to ±15 gauss.

The critical torque magnetic anisotropy measurements were carried out using an apparatus and methodology described elsewhere [22, 30].

Results

The powder epr spectrum of $Co(iPr\text{-}sal)_2$ is shown in Fig. 1. The low-field peak corresponds to g_1 = 7.09 while the high-field inflection yields g_2 = 0.57. No further signals were observed at fields up to 20,000 gauss, setting an upper limit on g_3 of 0.3.

Cobalt(II) doped $Zn(iPr\text{-}sal)_2$ has cell dimensions estimated from layer line spacings of oscillation photographs which correspond closely to the cell dimensions (a = 13.219(6); b = 19.697(8); c =

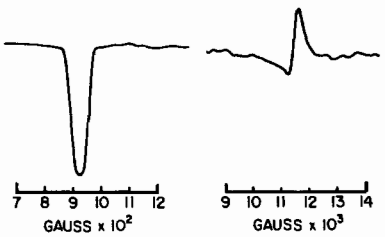

Fig. 1. Powder epr spectrum (4.2 K) of Co(iPr-sal)$_2$ diluted 1:100 in corresponding zinc complex taken at 9.182 GHz.

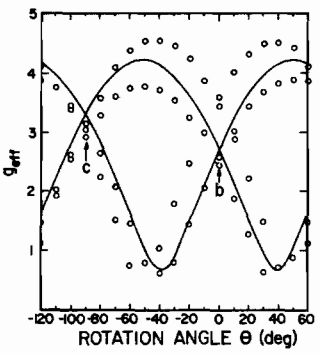

Fig. 2. Angular variation of the observed g-values for a single crystal of Co(iPr-sal)$_2$ (diluted 1:100 in corresponding zinc complex) as a function of rotation about the *a* crystallographic axis (*a*, vertical; *H*, horizontal).

15.140(18)) of the isomorphous nickel complex which crystallizes in the orthohombic space group, P_{bca} with 8 molecules in the unit cell [9]. These molecules occur in 4 magnetically equivalent pairs, the members of each pair being related by the center of symmetry. A general orientation of a crystal in a magnetic field should result in four distinct signals and this is observed. For orientations of the crystal with the magnetic field lying in one of the principal planes (100, 010, or 001), only two signals should be observed while when the magnetic field is parallel to a principal crystallographic axis only a single signal should be observed. The unavoidable orientation errors (<3°), coupled with the extremely large g-tensor anisotropy (*vide infra*) cause the general observation of four signals, none of which exhibit any indication of nuclear hyperfine structure. As the crystals are rotated with a principal crystallographic axis approximately vertical (H horizontal), four epr signals are observed which travel as pairs and approximately coalesce every 90° when a crystallographic axis becomes approximately parallel to the magnetic field. Figures 2, 3, and 4 show the observed angular variation of the observed g-values as a function of rotation about the *a*, *b*, and *c* crystallographic axes respectively. The results are presented as a plot of g_{eff} *vs.* θ, where θ is the rotational angle and g_{eff} is defined by: $h\nu = g_{eff}\beta H$ where h is Plank's constant, ν is the spectrometer frequency, β is the Bohr

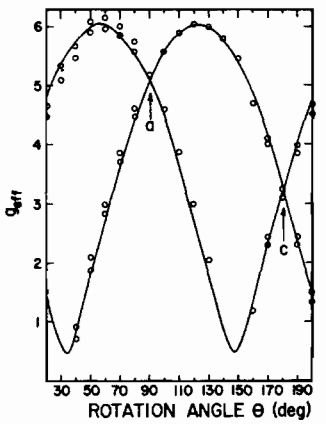

Fig. 3. Angular variation of the observed g-values for a single crystal of Co(iPr-sal)$_2$ as a function of rotation about the *b* crystallographic axis.

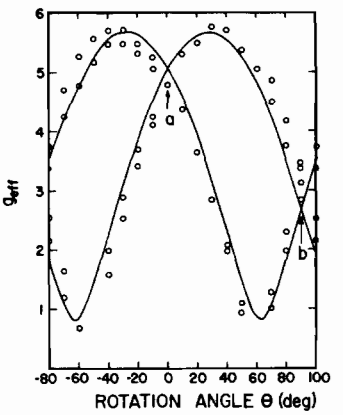

Fig. 4. Angular variation of the observed g-values for a single crystal of Co(iPr-sal)$_2$ as a function of rotation about the *c* crystallographic axis.

magneton, and H is the magnetic field strength in gauss.

The principal magnetic susceptibility anisotropies of orthorhombic single crystals of Co(iPr-sal)$_2$, measured at 298 K, are $\Delta\chi_a$ = 7.05; $\Delta\chi_b$ = 888.7; $\Delta\chi_c$ = 895.8 VVk/mol (1 VVk = 10^{-6} cgsu [30]; the subscript indicates the crystallographic axis held vertical in the experiment). Taking the average susceptibility χ = 8309 VVk/mol, corresponding to μ_{eff} = 4.45 μ_B [31] and the observation that $\chi_a > \chi_c > \chi_b$, the following principal crystal susceptibilities were calculated: χ_a = 8904, χ_b = 8008, χ_c = 8015 VVk/mol.

Analysis of the EPR Data

Schonland [32] has presented a general method for the determination of the principal values and directions of the g-tensor of a paramagnetic complex in a single crystal from measurements of g-value variation in three different crystallographic planes.

The variation of the effective g-value, g_{eff}, in each plane is described by eqn. 1.

$$g_{eff}^2 = \alpha_i + \beta_i \cos 2\theta + \gamma_i \sin 2\theta, \quad (1)$$

where θ is the angle of rotation about a vertical axis (the magnetic field H is horizontal) and the subscript i represents the crystallographic axis (*a*, *b*, or *c*) most nearly vertial. Owing to the unavoidable orientation errors, the data consists of signals which travel in pairs. The g-values for each pair were averaged and the constants α_i, β_i, and γ_i where obtained from a least squares fit to the data. The following numerical values were obtained: $\alpha_a = 9.19$; $\beta_a = -1.80$; $\gamma_a = 8.49$; $\alpha_b = 18.3$; $\beta_b = -7.30$; $\gamma_b = \pm 16.5$; $\alpha_c = 16.5$; $\beta_c = 9.10$; $\gamma_c = \pm 12.9$. The calculated g-value variation as a function of rotation angle θ using these parameters corresponding to the three equations 1, (i = *a*, *b*, *c*) are shown in Figs. 2, 3, and 4, respectively, Schonland [32] gives equations relating the parameters α_i, β_i, γ_i to the elements of a 3 X 3 matrix, A. Diagonalization of A according to eqn. 2 yields the principal g-values, g_x, g_y, and g_z.

$$\begin{bmatrix} g_x^2 & 0 & 0 \\ 0 & g_y^2 & 0 \\ 0 & 0 & g_z^2 \end{bmatrix} = \begin{bmatrix} \\ \tilde{\mathbf{P}} \\ \\ \end{bmatrix} \begin{bmatrix} \\ \mathbf{A} \\ \\ \end{bmatrix} \begin{matrix} x\ y\ z \\ \begin{bmatrix} \\ \mathbf{P} \\ \\ \end{bmatrix} \end{matrix} \begin{matrix} \\ a \\ b \\ c \end{matrix} \quad (2)$$

P is the 3 X 3 matrix of direction cosines of the principal g value axes (x, y, z) with respect to the principal crystallographic axes (*a*, *b*, *c*). Using the above values of α_i, β_i, and γ_i, the elements of the symmetric matrix **A** were determined as follows: $A_{11} = 25.58$; $A_{12} = 12.93$; $A_{13} = 16.52$; $A_{22} = 7.38$; $A_{23} = -8.49$; $A_{33} = 10.99$. Diagonalization of **A** according to eqn. 2 yields the following g-values: g_x, 6.56(0.06); g_y, 0.83(0.45); g_z, 0.47(0.62), where the numbers in parentheses represent probable rms errors determined according to the methods of Schonland [32]. These g-values are only in rough agreement with those extracted from the powder spectrum (7.09, 0.57 and <0.3). Furthermore, the direction cosine matrix P which achieves the diagonalization of A predicts that none of the principal magnetic axes come within 20° of the approximate C_2 axis of the Co(iPr-sal)$_2$ complex, a physically unlikely result for a molecular complex of this type. We attribute both of these difficulties to the unavoidable orientation errors associated with the experiment. Owing to the extremely large g-tensor anisotropy possessed by the complex, even small orientation errors can cause a noticeable effect on the derived parameters. Since it is our intention to map out the general features of the ground state magnetic properties of the present CoN_2O_2 chromophore, rather than to achieve a high level of accuracy for the values of the derived parameters, we have chosen to proceed with our analysis in the following manner. The g-values measured on the powder were taken to be correct. The value of g_z was set equal to 0.0 although virtually identical results are obtained when it is taken as 0.3. The approximate molecular C_2 axis was taken as the principal z axis and assigned direction cosines calculated from the structural results. We then sought, using eqn. 2, the orientation of the x and y principal axes which yields an A matrix most nearly identical (in a least squares sense) to that found in our experiment. We did this by starting with the direction cosine matrix *arbitrarily* assigned by Gerloch and Slade [33] to the orientation of the susceptibility tensor of Ni(iPr-sal)$_2$ which satisfied the condition that z ≡ C_2. The coordinate system was then rotated about the C_2(z) molecular axis in increments of several degrees. It was found that of the A matrices so obtained, the one most nearly in agreement with the experimental A matrix had associated with it a P matrix given below, eqn. 3.

TABLE I. Coordinates of Ligand Atoms (A) in the Coordinate System of the Principal g-Values.

Ligand atom	x	y	z
O(1)	−1.337	1.013	0.875
O(2)	1.362	−0.994	0.873
N(1)	−1.307	−1.161	−0.951
N(2)	1.243	1.131	−0.991

$$\mathbf{P} = \begin{matrix} \\ a \\ b \\ c \end{matrix} \begin{matrix} x \quad\quad y \quad\quad z \\ \begin{bmatrix} 0.7388 & 0.1861 & 0.6477 \\ -0.4130 & 0.8844 & 0.2171 \\ -0.5325 & -0.4280 & 0.7303 \end{bmatrix} \end{matrix} \quad (3)$$

In the course of these calculations the final column of the **P** matrix was left unchanged consistent with the assumed coincidence of the z principal molecular magnetic axis with the molecular C_2 axis. The first two columns of matrix **P** were varied according to rotational increments about the z axis. The best agreement between observed and calculated A matrices is obtained for a rotation of 4° from the arbitrary starting point. The degree of agreement between observed and calculated A matrices is a very strong function of the rotational angle. This allows us to have a good deal of confidence that the principal magnetic axes directions that we have determined are approximately correct. Matrix **P** used in conjunction with the atomic coordinates taken from the crystal structure [9], yields the coordinates of the ligand atoms in the principal molecular magnetic axis coordinate system given in Table I.

The orientation of the principal magnetic axes with respect to the atoms in the first coordination sphere is shown in Fig. 5. The x principal magnetic

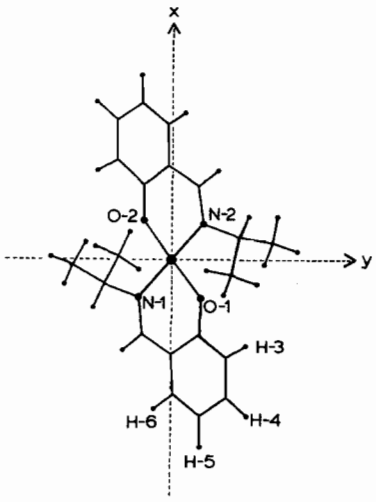

Fig. 5. Plan view down the approximate molecular $C_2(z)$ axis showing the orientation of the x and y magnetic axes with respect to the ligand atoms of Co(iPr-sal)$_2$. The labeling of the nitrogen and oxygen atoms corresponds to those given in ref. 9 from which the atomic coordinates were taken. The labeling of the hydrogen atoms corresponds to that used in the nmr studies (refs. 49 and 50).

axis approximately bisects the N–Co–O angle of each of the chelating ligands. This corresponds roughly to bisection of each of the ligand–metal–ligand angles of the distorted tetrahedral chromophore, the assumption made by Gerloch and Slade in their original choice of magnetic axis orientation in the corresponding nickel system. Further evidence supportive of the general correctness of this orientation comes from the AOM ligand field calculations described in the next section.

Ligand Field (AOM) Calculations of the Directions of the Principal Magnetic Axes

Owing to the fact that metal ion sites in proteins generally exhibit little or no symmetry, we have embarked on a program intended to develop a ligand field formalism suitable for such systems. In particular, we sought a ligand field model and computational methodology capable of predicting the *directions* of the magnetic axes in complexes devoid of symmetry. Earlier theoretical papers from this laboratory [18, 34, 35] have made a start in this direction. Very recently we have shown [18] that the angular overlap model [36–39], AOM, shows some potential for dealing with problems of this type. The spectral and magnetic (g- and susceptibility tensors) properties of two differently distorted $CoCl_4^{2-}$ ions have been satisfactorily accounted for [18] using a single AOM sigma parameter, e_σ. The AOM is bassed on a realistic picture of covalent binding and, although it is parametrized, it is directly related to structure in the sense that it requires a knowledge of the angular distribution of ligand atoms in the first coordination sphere of the metal ion. Only an outline of our computational procedure will be given as it has been presented in detail elsewhere [18].

The calculation of spectral and magnetic properties of Co(iPr-sal)$_2$ was carried out in the weak field formalism and includes spin–orbit coupling. The basis set was comprised of the forty spin–orbital components of the ^4F and ^4P terms of the d^7 (three vacancy) configuration, which were expressed in Slater determinantal form. A 40 × 40 perturbation matrix was computed with the ligand (AOM), V_{AO}, and spin–orbit coupling, $\lambda k\hat{L}\cdot\hat{S}$, perturbations applied simultaneously, where λ is the many-electron spin–orbit coupling constant and k is the orbital reduction factor. Both λ and k were taken to be isotropic in the present calculation. The quantity 15B (B is Racah's parameter) was added to the diagonal elements of the excited ^4P state. The ligand field aspect of the problem amounted to computing matrix elements of the type $\langle L, M_L|\hat{V}_{AO}|L', M_L'\rangle$, which comprise a 10 × 10 matrix which describes the orbital splitting of the ^4F and ^4P free ion states. These matrix elements were calculated from the one-electron matrix elements of the type: $\langle m_l|\hat{V}_{AO}|m_l'\rangle$, where the basis functions, $|m_l\rangle = |2\rangle, |1\rangle, |0\rangle, |-1\rangle, |-2\rangle$ are the five 3d orbitals in complex form. These matrix elements, in turn, were obtained from the AOM matrix elements, $\langle d_i|V_{AO}|d_j\rangle$, which are computed in a real d-orbital basis: $d_i = d_{z^2}, d_{yz}, d_{xz}, d_{xy}, d_{x^2-y^2}$ and are given by eqn. 4

$$\langle d_i|V_{AO}|d_j\rangle = \sum_{k=1}^{N} e_\sigma(k)S(d_i, \sigma_k)S(d_j, \sigma_k), \qquad (4)$$

where the sum is taken over the N ligands, $e_\sigma(k)$ is an adjustable energy parameter denoting the strength of the metal–ligand σ interaction, $S(d_i, \sigma_k)$ represents the angular part of the overlap integral between the real d-orbital d_i, and a σ-function, σ_k on the kth ligand. Given a particular coordination geometry, the values of $S(d_i, \sigma_k)$ are fixed since they depend only on the angular (spherical harmonic) properties of the individual d-orbitals and the angular distribution of ligand atoms. Hence e_σ is the only *adjustable* parameter used in defining the ligand field. The AOM may be generalized to include π- and δ-type interactions as well [36]. For cylindrically symmetric ligand a π-type interaction introduces an additional energy parameter $e_\pi(k)$ for each kind of ligand.

Schäffer [38] has described the analytical form of $S(d_i, \sigma_k)$ integrals and has outlined an elaborate matrix algebraic method for the computation of the one-electron matrix elements. $\langle d_i|\hat{V}_{AO}|d_j\rangle$. His procedure is readily adapted for machine computation. Further details of the method and a listing of the computer program used by us can be found elsewhere [40]. The one-electron part of the present calculation involves the complex d-orbital basis denoted by the column vector m_l which is related

TABLE II. Ligand Atom Coordinates (A) for Initial AOM Calculation ($\theta = 0°$).

Atom	*x*	*y*	*z*
O(1)	−1.263	1.104	0.875
O(2)	1.290	−1.087	0.873
N(1)	−1.385	−1.067	−0.951
N(2)	1.319	1.042	−0.991

to the real d-orbital basis **d** by the unitary transformation, **T**.

$$\mathbf{d} = \mathbf{T}\mathbf{m}_l \tag{5}$$

Thus the required 5 X 5 matrix, $V_{AO}^{complex}$, may be obtained from V_{AO}^{real} by the similarity transformation,

$$V_{AO}^{complex} = T^{\dagger} V_{AO}^{real} T \tag{6}$$

The eigenvalues of the 40 X 40 perturbation matrix in the $|L, M_L, S, M_S\rangle$ basis occur in pairs (Kramers doublets). Magnetic properties (molecular susceptibilities and g-values) were calculated by evaluating matrix elements of the Zeeman operator $k\hat{L}_\alpha + 2\hat{S}_\alpha$, $\alpha = x, y,$ or z between the eigenfunctions resulting from diagonalization of the 40 X 40 matrix. The principal molecular susceptibilities were calculated using the Van Vleck equation including both first- and second-order Zeeman contributions [30]. The g-values are defined by the equation: $h\nu = g_\alpha \beta H$, where ν is the spectrometer frequency, β is the Bohr magneton, and H is the magnetic field strength in gauss.

It may be of interest to note that while the elements of V_{AO}^{real} are real, the elements of $V_{AO}^{complex}$ may be either real or complex. They will be real in cases where the principal magnetic axes are defined by symmetry, while they will generally be complex in situations where symmetry does not specify the directions of all of the principal magnetic axes. The present complex of (approximate) C_2 symmetry represents such a case. The C_2 axis defines the z principal axis, but the orientation of the x and y axes in the perpendicular plane are not symmetry-specified. Our epr experiments were designed to determine these directions experimentally, while in this section we explore the ability of theory to predict these directions. In order to achieve this aim, our computer program [40] was written to handle complex arithmetic.

Our purpose was to see if the AOM in its *simplest* form is capable of qualitative agreement with the magnitudes of the principal components and the orientation of the experimental g-tensor of the lowest Kramers doublet. In order to do this, AOM ligand field calculations were carried out using the atomic coordinates of the nitrogen and oxygen ligand atoms from the crystal structure [9], but converting to a coordinate system with the metal atom at the origin and the approximate molecular C_2 axis taken as the z axis. The initial orientation of the x and y axes corresponds to the susceptibility tensor orientation chosen by Gerloch and Slade [33]. The coordinates of the ligand atoms for this initial orientation of the axes ($\theta = 0°$) are shown in Table II. AOM calculations were then carried out as the coordinate system was rotated about the z axis in 10° increments. The results for the calculated values of g_x and g_y for the lowest lying Kramers doublet are shown in Fig. 6. A positive value of θ corresponds to a coordinate system shift represented by the change in atomic coordinates from those given in Table II toward those given in Table I. The theoretical prediction of the directions of the magnetic axes occurs when the two g-values in the x, y plane are at their respective maxima and minima. Refining the rotational increments to 1°, we found this to occur at about $\theta = 2°$. This purely theoretical result is in excellent agreement with our experimental epr determination which occurs at $\theta = 4°$. After this work was complete [40] Gerloch and McMeeking [19] presented a computational AOM scheme different in methodology, but apparently equivalent to ours mathematically, for the location of magnetic axes in low symmetry complexes. Their method was applied to Ni(iPr-sal)$_2$ with the result that the magnetic axes were calculated to lie very close to the arbitrary orientation assigned earlier by Gerloch and Slade [33]. Their result further supports the essential correctness of our conclusions regarding the orientation of the magnetic axes in Co(iPr-sal)$_2$.

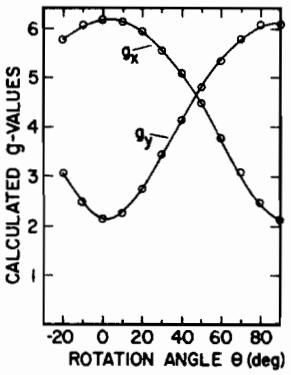

Fig. 6. Plot of the computed values of g_x and g_y from AOM calculations as a function of rotation of the ligand atom coordinates about the molecular $C_2(z)$ axis of Co(iPr-sal)$_2$ (see text).

It should be emphasized that for these calculations the *simplest* possible AOM scheme was adopted and no attempt was made to achieve exact agreement with experimental results through parameter adjustment or refinement of the model. A single AOM

TABLE III. Dipolar NMR Shifts[a] for the Protons of $Co(iPr\text{-}sal)_2$ Evaluated from Susceptibility Anisotropy Data and Derived Contact Shifts.

Proton	$(\Delta H^{ax}/H)^b$	$(\Delta H^{eq}/H)^c$	$(\Delta H^{dip}/H)$	$(\Delta H^{iso}/H)^d$	$(\Delta H^{con}/H)$
3-H	−5.6	−3.5	−9.1 ± 2.6	17.4	26.5
4-H	−4.0	−6.0	−10.0 ± 0.5	−47.1	−37.1
5-H	−4.4	−8.6	−13.0 ± 0.4	10.6	23.6
6-H	−7.3	−16.0	−23.3 ± 2.2	−36.9	−13.6
N=CH	−11.5	−21.7	−33.2 ± 7.9	−422	−389

[a]In ppm at 298 K, a negative sign represents a downfield shift. [b]Contribution of first term of eq. 8. [c]Contribution of second term of eq. 8. [d]From ref. 49.

sigma bonding parameter, e_σ, of 5000 cm^{-1} was used for both nitrogen and oxygen atoms. The following values of the other parameters were employed: λ, −172 cm^{-1}; k, 0.90; B, 960 cm^{-1}. The calculated energy levels are, of course, independent of rotation of the coordinate system and predict a zero-field splitting of the lowest $^4A_2$ state of T_d parentage of 19.2 cm^{-1}. Excited levels consist of Kramers doublets in the following energy ranges: 4108–5569 cm^{-1} (4); 8175–11006 cm^{-1} (8); 21795–23036 cm^{-1} (6), where the number in parenthesis designates the number of doublets in each range. These results are consistent with the observed broad, ill-resolved electronic absorption spectra [41, 42], although use of a lower value of B would improve agreement with the transitions corresponding to $^4A_2(F) \rightarrow {}^4T_1(P)$ (of T_d), which are calculated to be somewhat too high in energy. For $\theta = 0°$ the calculated g-values: $g_x = 6.19$; $g_y = 2.16$; $g_z = 1.52$ are in qualitative agreement with those observed: 7.09, 0.57, and <0.3, respectively. No attempt was made to refine the parameter choice or to extend the model (such as to include different e_σ parameters for nitrogen and oxygen ligand atoms or to include π-type interactions). Our purpose was to assess the utility of theory at the simplest possible level to predict directions of the principal magnetic axes. The curves of the calculated principal magnetic susceptibility components, χ_x and χ_y, parallel the behavior of the g-values shown in Fig. 6 and maximize and minimize at the same angular positions. This is true of both first- and second-order Zeeman contributions. Only a 45° angular range of the calculations is unique and the curves are mirror images with respect to a vertical line drawn through the cross-over point, since the assignment of the x or y label to a particular curve represents an arbitrary choice of coordinate system.

Principal Molecular Susceptibilities and Evaluation of Dipolar NMR Shifts

Single crystal susceptibility anisotropy measurements can establish only the values of the principal crystal susceptibilities, χ_a, χ_b, and χ_c along the orthogonal crystal axes for an orthorhombic crystal. In order to extract the magnitudes of the principal *molecular* susceptibilities, knowledge of the orientation of the principal molecular magnetic axes with respect to the crystal axes is required. In the present case this knowledge is provided by the single crystal epr results as corroborated by the AOM calculations. Using the elements of the **P** matrix (eqn. 3), the principal molecular susceptibilities χ_x, χ_y, and χ_z were determined by solving, simultaneously, eqns. 7 [30].

$$\chi_a = \chi_x P_{11}^2 + \chi_y P_{12}^2 + \chi_z P_{13}^2$$
$$\chi_b = \chi_x P_{21}^2 + \chi_y P_{22}^2 + \chi_z P_{23}^2 \quad (7)$$
$$\chi_c = \chi_x P_{31}^2 + \chi_y P_{32}^2 + \chi_z P_{33}^2$$

The results (298 K) are $\chi_x = 10599$, $\chi_y = 7515$ and $\chi_z = 6813$ VVk/mol. Using these results the dipolar contribution $(\Delta H^{dip}/H)$ to the nmr isotropic shifts $(\Delta H^{iso}/H)$, of $Co(iPr\text{-}sal)_2$ in solution may be evaluated using eq. 8 [21–25].

$$\left(\frac{\Delta H}{H}\right)^{dip} = -\frac{1}{3N}\left[\chi_z - \frac{1}{2}(\chi_x + \chi_y)\right]\left[\frac{3\cos^2\theta - 1}{r^3}\right] - \frac{1}{2N}[\chi_x - \chi_y]\left[\frac{\sin^2\theta\cos 2\phi}{r^3}\right] \quad (8)$$

where N is Avogadro's number and r, θ, and ϕ are the spherical polar coordinates of the resonating nucleus. The results for the protons of $Co(iPr\text{-}sal)_2$ are shown in Table III (see structure **1** and Fig. 5 for the numbering system) along with the contact shifts, $(\Delta H^{con}/H)$, derived from the relationship: $(\Delta H^{iso}/H) = (\Delta H^{dip}/H) + (\Delta H^{con}/H)$.

The shifts were calculated using the atomic positional coordinates of ref. 9 and averaging the very similar results for protons related by the approximate molecular C_2 axis. The uncertainties listed under $(\Delta H^{dip}/H)$ represent the results of calculations in which the directions of the x and y molecular magnetic axes were rotated by ±5° about the molecular $C_2(z)$ axis. The calculated dipolar shifts for the methine and methyl protons of the isopropyl group

are +14.5 and +32.1 ppm, respectively, for these protons fixed in their solid state orientations. These numbers should be regarded as rough estimates only, since no rotational averaging has been taken into account. Nevertheless the +32.1 ppm dipolar shift calculated for the methyl resonance would appear to account in large measure for the observed upfield shift (+26.3 ppm).

Discussion

EPR Results

Surprisingly little epr data is available for high-spin, four-coordinate cobalt(II) complexes. Most of the early work is devoted to the study of the tetrahedral or very slightly distorted tetrahedral $Co^{II}X_4$ coordination unit [43, 44], where X represents a halide or chalconide ligand. Attempts to understand the epr spectra of cobalt(II) in zinc metalloenzymes have depended upon comparison with the spectra of low-symmetry model compounds of various coordination numbers [16]. The only four-coordinate model complexes for which data are currently available [16, 45–48] contain the $Co^{II}N_2X_2$ or $Co^{II}NX_3^-$ coordination units where X is a halide ion and the nitrogen ligand atom is supplied by a pyridine, quinoline, or aniline derivative. There is a good degree of similarity in appearance of the epr spectra of certain of these model complexes to particular cobalt(II)-substituted enzymes, *e.g.*, carboxypeptidase [16], thermolysin [16], carbonic anhydrase [17]. With the exception of $[Co(quinoline)Br_3]^-$ [48], all of the model complexes so far examined were studied as powders or frozen solutions and, therefore, did not yield information regarding the relationship of the magnetic axes to the structure of the first coordination sphere. We sought to gain additional insight into the use of cobalt(II) as a reporter ion for distorted protein environments by initiating a study of cobalt(II) complexes involving ligand atoms found in biological systems. We wished to establish, *via* single crystal studies, the relationship between the coordination geometry and the g-tensor orientation.

Ironically, the g-values determined for the present $Co(iPr\text{-}sal)_2$ complex with its CoN_2O_2 coordination sphere are less similar to those of cobalt substituted carboxypeptidase and thermolysin [16], which most likely contain this chromophore, than are certain of the cobalt(II) model complexes which contain halide ligands. This fact, however, should serve as an important caution to those wishing to draw firm conclusions regarding the nature and structure of a cobalt(II) coordination sphere from a simple inspection of its associated epr spectrum. The g-tensor of $Co(iPr\text{-}sal)_2$ is more anisotropic than is that of any other cobalt(II) complex so far investigated. This occurs even though a naive consideration of relative ligand field strengths: N *vs.* O in $Co^{II}N_2O_2$, against N *vs.* X in $Co^{II}N_2X_2$, X = halide, might suggest otherwise. Clearly the g-tensor is distorted tetrahedral cobalt(II) complexes is extremely sensitive to environment. However, until further data are in hand, the relative importance of various factors (*e.g.*, angular distortion *vs.* diverse ligand field strengths) cannot be assessed.

Although unavoidable orientation errors in our single crystal experiments prevented the accurate determination of g-values, the extremely large g-tensor anisotropy allowed us to determine the orientation of the g-tensor with a reasonable degree of confidence. Our complex possesses approximate C_2 symmetry and we find the minimal g-value ($g_z < 0.3$) lies along the direction of the approximate C_2 axis. The other two principal magnetic axes were found to lie quite close to what correspond to the other C_2 axes of idealized T_d symmetry (rather than lying in the σ_d planes which might not have been unreasonable). It is perhaps noteworthy that the axis of *largest* g-value ($g_x = 7.09$) roughly bisects the smallest ligand–metal–ligand angles (~94°) which are provided by the restricted bite of the individual salicylaldimine ligands. The axis of intermediate g-value ($g_y = 0.57$) nearly bisects the angles (112–113°) defined by nitrogen and oxygen atoms of different chelate ligands, while the axis of lowest g-value ($g_z < 0.3$) bisects the largest angles in the coordination sphere, namely O–Co–O and N–Co–N angles of 125° and 121°, respectively. Whether or not a correlation will hold in general between magnetic axis directions and g-value magnitudes and the directions of angle bisectors and the magnitudes of the angles subtended by adjacent ligand atoms, must await further experimentation with single crystals.

In keeping with the usual situation in tetrahedral or distorted tetrahedral cobalt(II), no cobalt nuclear hyperfine structure is apparent in either our single crystal or powder spectra. An interesting experimental aspect is that the smallest g-value was not observable experimentally. The powder spectrum is ambiguous on this point and, by itself, could have been interpreted as being axially symmetric with $g_\parallel = 7.09$ and $g_\perp = 0.53$. The single crystal spectra, however, demand an additional g-extremum at fields higher than obtainable with our instrument. This result presents yet another caution in the interpretation of powder and frozen-solution epr spectra of four-coordinate, high-spin cobalt(II) complexes.

AOM Calculations

Phenomenological ligand field theory, LFT, which has been so successful in furthering our understanding of the spectra and magnetic properties of high-symmetry transition metal complexes, becomes less and less useful as symmetry is diminished. This is because more and more parameters, devoid of physical inter-

TABLE IV. Dipolar NMR Shifts[a] and Derived Contact Shifts for the Protons of Ni(iPr-sal)$_2$ Evaluated from Susceptibility Anisotropy Data, and Contact and Isotropic Shift Ratios for the Cobalt and Nickel Complexes.

Proton	$(\Delta H^{ax}/H)^b$	$(\Delta H^{eq}/H)^c$	$(\Delta H^{dip}/H)$	$(\Delta H^{iso}/H)^d$	$(\Delta H^{con}/H)$	Shift Ratios[e]			
						Co^{iso}	Ni^{iso}	Co^{con}	Ni^{con}
3-H	0.7	2.2	2.9	23.7	20.8	1.64	1.00	1.12	1.16
4-H	0.5	3.7	4.2	−19.0	−23.2	−4.44	−0.80	−1.57	−1.30
5-H	0.5	5.3	5.8	23.7	17.9	1.00	1.00	1.00	1.00
6-H	0.9	9.8	10.7	−3.7	−14.4	−3.48	−0.16	−0.58	−0.80
N=CH	1.4	13.3	14.7	−328[f]	−343	−39.8	−13.8	−16.5	−19.2

[a]In ppm at 295 °K, a negative sign represents a downfield shift. [b]Contribution of first term of eq. 8. [c]Contribution of second term of eq. 8. [d]From ref. 50, represents shifts of fully tetrahedral form. [e]Shift of 5-H resonance normalized to 1.00. [f]Estimated from data on 5-CH_3 derivative in footnote 31b of R. H. Holm, A. Chakravorty, and G. O. Dudek, *J. Am. Chem. Soc., 86,* 379 (1964), taking into account the small temperature difference and position of planar–tetrahedral equilibrium. [g]Dipolar shifts for isopropyl C–H and CH_3 protons calculate to be −8.4 and −18.4 ppm, respectively.

pretability, are required to describe the experimental observables. LFT has been applied to the $Co^{II}L_2X_2$ chromophore [17, 45, 47], however since it has no predictive capacity, little or no physical insight was achieved.

In 1972 one of us presented a ligand field calculational method [34], applicable to systems devoid of symmetry, of applying the results of one-electron molecular orbital, MO, theory of transition metal complexes to many-electron LF calculations of spectral and magnetic properties. This procedure, which was called the "effective perturbation method", has as its input the energies and eigenfunctions of the "mainly d" MOs of a complex. As a corollary of this method it was shown [35], for complexes belonging to many, but not all, point symmetries, that the one-electron d-orbital energies themselves may serve as LF parameters. We feel, however, for an analysis of metalloenzyme systems, that the parameterized AOM, which is based on a realistic bonding model and structural relationships, is the most promising. In a recent paper [18] we have shown that the AOM can successfully account for the spectral and magnetic properties of distorted tetrahedral $CoCl_4^{2-}$ ions with a minimum number of adjustable parameters. In the present paper, a calculation of this sort is extended to predict the directions of the principal magnetic axes as well as the magnitudes of various observable quantities. It should be emphasized that we chose the *simplest* possible model with only four adjustable parameters: e_σ, k, λ, B. Further refinement of the theoretical model to achieve more exact agreement with experimental magnitudes will be the subject of future research. Preliminary results indicate that the predicted directions of the magnetic axes are independent of the choice of e_σ parameter values. Thus, the virtually exact agreement between predicted and observed g-tensor orientation is extremely gratifying.

NMR Dipolar Shifts

A comparison of the dipolar nmr shifts calculated from the susceptibility anisotropy data with the observed isotropic shifts [49] (Table III) shows that the former make significant contributions and must be taken into account in evaluating the Fermi contact contributions to the shifts. It is the Fermi contact shifts, of course, which reflect the distribution of unpaired electron spin density in the coordinated ligand. In this context it is appropriate to reevaluate the dipolar and contact shifts of the analogous nickel system, Ni(iPr-sal)$_2$. Benelli *et al.* [50], employing the earlier anisotropy data of Gerloch and Slade [33], calculated dipolar shifts (300 °K) using eq. 8 for the 3-H, 4-H, 5-H, and 6-H resonances of −1.4, 2.3, 4.5, and 8.4 ppm, respectively. Using the more recent magnetic data of Cruse and Gerloch [20] and the orientation of the magnetic axes found here (which corresponds closely to that calculated by Cruse and Gerloch [20]), we calculate dipolar shifts of the protons of Ni(iPr-sal)$_2$ shown in Table IV. A comparison of Tables III and IV reveals that the dipolar shifts of the nickel complex are 1/3 to 1/2 as large as those of the cobalt complex and opposite in sign. This accounts in some measure for the apparent success of most early interpretations of isotropic shifts in pseudotetrahedral nickel complexes as being Fermi contact in origin. It is also in accord with theoretical calculations of ours [51], with solution nmr studies [49] of the interaction of nitroaromatic molecules with N-alkyl salicylaldehyde complexes of cobalt(II), nickel(II), and copper(II), and with susceptibility anisotropy studies [22] on $M[(C_6H_5)_3P]_2Cl_2$, M = Co, Ni complexes. The isotropic and contact shift ratios given in Table IV reveal that while the observed isotopic shift ratios differ markedly for cobalt and nickel, the contact shift ratios for the two systems are much more similar. This results implies a similar unpaired

TABLE V. Dipolar shifts (ppm at 298 K) to be Expected for Nuclei Situated at Various Distances, r, from the Metal Along the Magnetic Axes of $Co(iPr\text{-}sal)_2$ and Metmyoglobin Cyanide[a], MbCN.

	Axis				
	r	5 A	10 A	15 A	20 A
$Co(iPr\text{-}sal)_2$	x	10.6	1.3	0.4	0.2
	y	−30.5	−3.8	−1.1	−0.5
	z	19.8	2.5	0.7	0.3
MbCN	x	13.5	1.7	0.5	0.1
	y	5.9	0.7	0.2	0.0
	z	−19.5	−2.4	−0.7	−0.2

[a]From ref. 52.

electron spin density distribution in the aromatic ligand of the cobalt and nickel complexes. Such a similarity has often been noted in the past and forms the basis for the "ratio method" [21] of separation of dipolar and contact contributions to observed shifts in axially symmetric hexacoordinate cobalt and nickel complexes.

From the point of view of using cobalt(II) as a nmr shift probe in place of zinc in metalloproteins, it is useful to have some idea of the strength of the dipolar field surrounding this ion. Since the dipolar interaction is a through-space rather than a through bond effect, it can affect nuclear resonances of nearby portions of the polypeptide chain that are not directly bound to the metal. Since the present complex is the most anisotropic of its type known, the dipolar field associated with it can provide a reasonable upper limit for the dipolar shift magnitudes to be expected for this class of probe ion (cobalt(II) in a distorted tetrahedral environment). In Table V are set out the dipolar resonance shifts that would be experienced by nuclei situated at various distances from the metal along the magnetic axes of the complex. It is evident that resonance shifts of up to 1 ppm are possible for nuclei as far away as 15 Å from the metal. For comparison purposes, the analogous shift values for the low-spin iron(III), d^5, prosthetic group of metmyoglobin cyanide [52, 53], MbCN, are also tabulated. Clearly, dipolar shifts produced by cobalt(II) in a distorted tetrahedral environment cannot be ignored and may be as large or larger than those produced by the paramagnetic center in the much-studied low-spin iron(III) heme proteins.

In summary, then, in a continuation of our attempts to understand in detail the magnetic properties of cobalt(II) in low-symmetry metalloenzyme site, we have examined single crystals of a complex containing the $Co^{II}N_2O_2$ chromophore and determined the g-values and directions of the principal magnetic axes. A theoretical prediction of g-tensor orientation, based on the application of the AOM, agrees well with experiment. $Co(iPr\text{-}sal)_2$ is the most highly anisotropic distorted tetrahedral cobalt(II) complex so far studied. The fact that its g-tensor anisotropy is larger than those of metalloenzymes containing the $Co^{II}N_2O_2$ coordination unit, suggest that considerable caution must be exercised when interpreting epr spectra of cobalt(II) substituted metalloproteins in terms of a particular coordination sphere composition or geometry. The dipolar shifts evaluated from the susceptibility anisotropy data on $Co(iPr\text{-}sal)_2$ are substantial and, when accounted for along with the smaller shifts of opposite sign of the analogous nickel complex, provide evidence for a similar pattern of spin delocalization in the two complexes. Dipolar shifts induced by cobalt(II) in distorted tetrahedral environments in metalloproteins are expected to be significant. Further experimental work and theoretical scrutiny is clearly necessary in order to gain a firm understanding of cobalt(II) bound to biological macromolecules.

Acknowledgment

This research was supported by the National Science Foundation through grant CHE76-08528.

References

1 B. L. Vallee and W. E. C. Wacker, 'Metalloproteins', in H. Neurath ed., 'The Proteins', Academic Press, N.Y., 2nd ed., Vol. V (1970).
2 J. F. Riordan, in R. E. Burch and J. F. Sullivan eds., 'The Medical Clinics of North America, Symposium on Trace Elements', W. B. Saunders, Phila. (1976), Vol. 60, No. 4, pp. 661–674.
3 A. S. Mildvan and M. Cohn, *Advan. Enzymol., 33,* 1 (1970).
4 S. Lindskog, *Struct. Bonding (Berlin), 8,* 153 (1970).
5 F. A. Quiocho and W. N. Lipscomb, *Adv. Protein Chem., 25,* 1 (1971).
6 B. W. Matthews, L. H. Weaver, and W. R. Kester, *J. Biol. Chem., 249,* 8030 (1974).
7 S. Lindskog, L. E. Henderson, K. K. Kanman, A. Liljas, P. O. Nyman and B. Strandberg, in 'The Enzymes', P. D. Boyer ed., Academic Press, N.Y. (1971) 3rd ed., Vol. V, pp. 587–665.
8 C.-I. Branden, H. Jornvall, H. Eklund, and B. Furugren, in 'The Enzymes', P. D. Boyer ed., Academic Press, N.Y. (1975) 3rd ed. Vol. XI, Part A, pp. 104–190.
9 M. R. Fox, P. L. Orioli, E. C. Lingafelter, and L. Sacconi, *Acta Crystallogr., 17,* 1159 (1964).
10 L. Sacconi, P. L. Orioli, P. Paoletti, and M. Ciampolini, *Proc. Chem. Soc.,* 256 (1962).
11 See for instance B. L. Vallee, J. F. Riordan, D. S. Auld, and S. A. Latt, *Philos. Trans. R. Soc. London, Ser. B., 257,* 215 (1970).
12 See for instance B. Holmquist, T. A. Kaden, and B. L. Vallee, *Biochem.,* 1454 (1975).
13 W. D. Benhnke and B. L. Vallee, *Proc. Nat'l. Acad. Sci. U.S.A., 69,* 2442 (1972).

14 S. A. Latt, D. S. Auld, and B. L. Vallee, *Biochem., 11,* 3015 (1972).
15 W. DeW. Horrocks, Jr., B. Holmquist, and B. L. Vallee, *Proc. Natl. Acad. Sci. U.S.A., 72,* 4764 (1975).
16 F. S. Kennedy, H. A. O. Hill, T. A. Kaden, and B. L. Vallee, *Biochim. Biophys. Res. Commun., 48,* 1533 (1972).
17 S. A. Cockle, S. Lindskog, and E. Grell, *Biochem. J., 143,* 703 (1974).
18 W. DeW. Horrocks, Jr., and D. A. Burlone, *J. Am. Chem. Soc., 98,* 6512 (1976).
19 M. Gerloch and R. F. McMeeking, *J. Chem. Soc. Dalton,* 2443 (1975).
20 D. A. Cruse and M. Gerloch, *J. Chem. Soc. Dalton,* 152 (1977).
21 W. DeW. Horrocks, Jr., *Inorg. Chem., 9,* 690 (1970).
22 W. DeW. Horrocks, Jr., and E. J. Greenberg, *Inorg. Chem., 10,* 2190 (1971).
23 W. DeW. Horrocks, Jr., and D. DeW. Hall, *Inorg. Chem., 10,* 2368 (1971).
24 W. DeW. Horrocks, Jr., and J. P. Sipe III, *Science, 177,* 994 (1972).
25 W. DeW. Horrocks, Jr., in G. N. La Mar, W. DeW. Horrocks, Jr. and R. H. Holm eds., 'NMR of Paramagnetic Molecules: Principles and Applications', Academic Press, N.Y. (1973) Chapter 4, pp. 128–177.
26 W. DeW. Horrocks, Jr., Chapter 12 in ref. 25, pp. 475–519.
27 I. D. Campbell, C. M. Dobson, and R. J. P. Williams, *Proc. R. Soc. London, Ser. A, 345,* 41 (1975).
28 R. M. Keller and K. Wüthrich, *Biochim. Biophys. Acta, 285,* 326 (1972).
29 H. Nishikawa, S. Yamada, and R. Tsuchida, *Z. Naturforsch., 17B,* 78 (1962).
30 W. DeW. Horrocks, Jr. and D. DeW. Hall, *Coord. Chem. Rev., 6,* 147 (1971).
31 B. O. West, *J. Chem. Soc.,* 1374 (1962).
32 D. S. Schonland, *Proc. Phys. Soc., 73,* 788 (1959).
33 M. Gerloch and R. C. Slade, *J. Chem. Soc. A,* 1022 (1969).
34 W. DeW. Horrocks, Jr., *J. Am. Chem. Soc., 94,* 656 (1972).
35 W. DeW. Horrocks, Jr., *Inorg. Chem., 13,* 2775 (1974).
36 C. E. Schäffer and C. K. Jørgensen, *Molec. Phys., 9,* 401 (1965).
37 C. K. Jørgensen, R. Pappalardo, and H. H. Schmidtke, *J. Chem. Phys., 39,* 1422 (1963).
38 C. E. Schäffer, *Struct. Bonding (Berlin), 5,* 68 (1968).
39 E. Larsen and G. N. La Mar, *J. Chem. Educ., 51,* 633 (1974).
40 D. A. Burlone, *Ph.D. Thesis,* The Pennsylvania State University (1975).
41 L. Sacconi, M. Ciampolini, F. Maggio, and F. P. Cavasino, *J. Am. Chem. Soc., 84,* 3246 (1962).
42 L. Sacconi, P. Paoletti, and M. Ciampolini, *J. Am. Chem. Soc., 85,* 411 (1963).
43 A. Abragam and B. Bleaney, 'Electron Paramagnetic Resonance of Transition Ions', Oxford University Press, London (1970).
44 B. R. McGarvey, *Transition Metal Chem., 3,* 89 (1966).
45 Yu. V. Yablokov, V. K. Voronkova, V. F. Shiskhov, A. V. Ablov, and Zh. Yu. Vaisbem, *Soviet Phys. Solid State Engl. Transl., 13,* 831 (1971).
46 V. K. Voronkova, M. M. Zaripov, and Yu. V. Yablokov, *Soviet Phys. Solid State Engl. Transl., 16,* 593 (1974).
47 V. K. Voronkova, M. M. Zaripov, Yu. V. Yablokov, A. V. Ablov, and M. A. Ablova, *Dokl. Phys. Chem. Engl. Transl., 214,* 42 (1974).
48 A. Bencini and D. Gatteshi, *Inorg. Chem., 16,* 2141 (1977).
49 H. A. O. Hill, A. D. J. Horsler, and P. J. Sadler, *J. Chem. Soc. Dalton,* 1805 (1973).
50 C. Benelli, I. Bertini, and D. Gatteschi, *J. Chem. Soc. Dalton,* 661 (1972).
51 W. DeW. Horrocks, Jr. and D. A. Burlone, unpublished calculations.
52 W. DeW. Horrocks, Jr. and E. S. Greenberg, *Biochim. Biophys. Acta, 322,* 38 (1973).
53 W. DeW. Horrocks, Jr. and E. S. Greenberg, *Molec. Phys., 27,* 993 (1974).